Distributed Stochastic Model Predictive Control with Taguchi's Robustness for Vehicle Platooning

Jianhua Yin, Dan Shen, *Student Member, IEEE*, Xiaoping Du, Lingxi Li, *Senior Member, IEEE*

***Abstract*—Vehicle platooning for highway driving has many benefits, such as lowering fuel consumption, improving traffic safety, and reducing traffic congestion. However, its performance could be undermined due to uncertainty. This work proposes a new control method that combines distributed stochastic model predictive control with Taguchi's robustness (TR-DSMPC) for vehicle platooning. The proposed method inherits the advantages of both Taguchi's robustness (maximizing the mean performance and minimizing the performance variation due to uncertainty) and stochastic model predictive control (ensuring a specific reliability level). Taguchi's robustness is achieved by introducing a variation term in the control objective to bring a trade-off between mean performance and its variation. TR-DSMPC propagates uncertainty via an approximation method: First-Order Second Moment, which is far more efficient than Monte Carlo-based methods. The uncertainty is considered from two perspectives, time-independent uncertainty by random variables and time-dependent uncertainty by stochastic processes. We compare the proposed method with two other MPC-based methods in terms of safety (spacing error) and efficiency (relative velocity). The results indicate that our proposed method can effectively reduce the performance variation and maintain the mean performance.**

***Index Terms*—Vehicle platooning, Taguchi's robustness, distributed stochastic model predictive control, uncertainty.**

NOMENCLATURE

C_a	Aerodynamic drag coefficient.
E	Mean control objective.
f	Rolling friction coefficient.
H	Random field.
N_p	The length of prediction horizon.
s	Vehicle position.
T	Vehicle torque.
u	Control signal.
V	Variation term of control objective.
v	Vehicle velocity.
Y	General model response.
$\boldsymbol{Z}$	Input random variables.
η	Mechanical efficiency coefficient.
μ	The mean value.
σ	The standard deviation.
τ	Inertial time lag.

**Corresponding author: Xiaoping Du.*

J. Yin and X. Du are with the Department of Mechanical and Energy Engineering, Purdue School of Engineering and Technology, Indiana University-Purdue University Indianapolis (IUPUI), 723 West Michigan Street, SL-260, Indianapolis, IN 46202, USA. E-mails: {jy57, duxi}@iu.edu.

D. Shen and L. Li are with the Transportation and Autonomous Systems Institute (TASI), also with the Department of Electrical and Computer Engineering, Purdue School of Engineering and Technology, Indiana University-Purdue University Indianapolis (IUPUI), 723 West Michigan Street, SL-160, Indianapolis, IN 46202, USA. E-mails: {danshen, LL7}@iupui.edu.

I. INTRODUCTION

AUTONOMOUS vehicle platooning for highway driving can improve traffic conditions by enhancing road safety, increasing highway utility efficiency, and improving fuel economy [1]–[3]. This is achieved by regulating the target vehicles to operate at desired speed under specific traffic conditions. Since the pioneering work in PATH project [4], [5] in California, many research topics have been studied, such as control policy [6], information flow topology [7], vehicle dynamics model [8], and homogeneity and heterogeneity [9]. Relative advanced control methods are developed with many successful applications [10]–[12].

Although considerable success has been achieved, challenges remain on the road toward safe and efficient platooning, such as uncertainty in vehicle dynamics [13], [14] and vehicle-to-vehicle (V2V) communications [15], [16]. Uncertainty could be from vehicle operation (time lag, mechanical efficiency, etc.), outside environment (road friction, air drag, etc.), and communication delay or packet drop, which may undermine the controller performance. Considering uncertainty is critical in controller design for successful platooning with guaranteed performance.

Model Predictive Control (MPC) [17] is an advanced control method and has been applied to diverse applications including vehicle platooning, with demonstrated exceptional performance [18], [19]. Based on the current status, MPC repeatedly solves an open loop Optimal Control Problem (OCP) along the prediction horizon at every time instant. However, MPC, which also is called nominal MPC, uses a deterministic approach without taking the uncertainty into account. The deterministic approach may be inadequate to deal with real situations since uncertainties always exist.

Robust MPC (RMPC) [20] is one type of MPC to handle uncertainty to improve control performance. RMPC uses min-max OCP formulation [15], [16] to minimize the worst case in all possible outcomes to ensure the control performance. For example, the study in [16] uses RMPC to address uncertainty in the dynamics model and V2V communications, which shows that RMPC outperforms the nominal MPC for the platooning task. This approach, however, has three drawbacks: 1) the control policy could be over-conservative or even possibly infeasible since the worst case rarely happens [21]; 2) finding the worst case introduces an additional computational cost that could be expensive, especially when multiple parameters exist; 3) RMPC assumes that the uncertainties are characterized by bounded distributions with finite outcomes, which is different from the probabilistic nature in the real

world. Using a probabilistic approach is more natural and realistic to characterize the uncertainties in control design.

Stochastic MPC (SMPC) [22] treats uncertainties in a probabilistic approach, thereby having a larger feasible design region without over-conservative issues compared to RMPC. Ju et al. [23] proposed a distributed SMPC (DSMPC) algorithm with recursive feasibility. The Monte Carlo Simulation (MCS) results show that DSMPC has a better average performance than distributed RMPC (DRMPC).

Apart from the MPC-based controllers, other advanced control strategies [24]–[26] are developed to improve the control performance in platooning. For example, an adaptive platooning strategy was proposed to account for bidirectional interaction of vehicles and engine cohesiveness in heterogeneous platoons with uncertainty [27]. A fully distributed event-triggered controller under intermittent communication was developed by Wu et al. [28]. And a distributed H-infinity control method was introduced in [29] for a multi-vehicle system considering dynamics model uncertainty.

Another method for design under uncertainty is Taguchi's robust design [30]. It has many successful applications in many fields [31]–[35] and can potentially improve the platooning control further. Taguchi's robustness minimizes the influence of uncertainty without eliminating its sources. The main idea is to balance the average control performance and its variation such that the controller is capable to handle different situations with smaller performance variations.

In [36], we proposed a preliminary concept regarding a new control strategy integrated with Taguchi's robustness. Now, we extend the novel control strategy with detailed algorithm formulation and comparison studies in this work. The main contributions are summarized below.

- A novel control strategy, TR-DSMPC, is proposed that combines Taguchi's robustness strategy and distributed SMPC to ensure both robustness and reliability.
- An approximation method called the First Order Second Moment (FOSM) [37] is used for uncertainty propagation. FOSM is far more efficient than Monte Carlo-based sampling methods [38]. Hence, the computational cost of the proposed approach is significantly reduced.
- Uncertainty in different road conditions is modeled by stochastic processes for vehicle control. This approach provides a more realistic and natural way to model road conditions that vary randomly and spatially.

The remainder of this paper is organized as follows. The control problem to be studied is formulated in Section II, including vehicle dynamics, information topology, FOSM, and Taguchi's robustness. The uncertainty modeling methods and the proposed optimization model are introduced in Section III. Numerical simulations and the comparison studies are presented and discussed in Section IV. Conclusions and future work are given in Section V.

II. Problem Formulation

We consider a longitudinal heterogeneous vehicle platoon as the application scenario as shown in Fig. 1. The platoon task includes $N+1$ vehicles (nodes), a leading vehicle (numbered by 0) and N followers (numbered by $1,\dots,N$). A nonlinear longitudinal dynamic model is utilized to characterize the vehicle dynamic motions. The platoon uses a Predecessor Following (PF) topology to simulate the information flow. Other information topologies also can be used, such as Predecessor-leader following (PLF) topology, and Bidirectional (BD) topology.

A. Model of Vehicle Dynamics

Each vehicle in the platoon is controlled with its own state (position, velocity, torque, etc.) and control signal with constraints. The vehicle longitudinal dynamics is characterized by a discrete time state-space representation shown below.

$$\begin{cases} s_i(k+1) = s_i(k) + v_i(k)\Delta t \\ v_i(k+1) = v_i(k) + \frac{\Delta t}{m_i}\left(\frac{\eta_i T_i(k)}{r_i} - C_{a_i} v_i(k)^2 - m_i g f_i\right) \\ T_i(k+1) = T_i(k) + \frac{\Delta t}{\tau_i}\left(u_i(k) - T_i(k)\right) \end{cases} \tag{1}$$

where s_i, v_i, T_i represent the position, velocity, and torque of the i-th vehicle, respectively; m_i, r_i are the mass and tire radius of the i-th vehicle, respectively; and η_i, C_{a_i}, f_i, and τ_i are the mechanical efficiency coefficient, aerodynamic drag coefficient, rolling friction coefficient, and inertial time lag of the i-th vehicle, respectively, which are uncertain parameters and influence the state of vehicles; u_i is the control input of the i-th vehicle; and g is the gravitational acceleration. We simplify Eq. (1) as

$$\boldsymbol{x}_i(k+1) = A_i \boldsymbol{x}_i(k) + B_i u_i(k) + \psi_i \tag{2}$$

where $\boldsymbol{x}_i = (s_i, v_i, T_i)^{\mathbf{T}}$, and

$$A_i = \begin{bmatrix} 1 & \Delta t & 0 \\ 0 & 1 - \frac{C_{a_i} v_i(k) \Delta t}{m_i} & \frac{\eta_i \Delta t}{m_i r_i} \\ 0 & 0 & 1 - \frac{\Delta t}{\tau_i} \end{bmatrix} \tag{3}$$

$$B_i = \begin{bmatrix} 0 \\ 0 \\ \frac{1}{\tau_i} \end{bmatrix} \tag{4}$$

$$\psi_i = \begin{bmatrix} 0 \\ -g f_i \Delta t \\ 0 \end{bmatrix} \tag{5}$$

Then the heterogeneous platoon dynamics model can be represented by

$$\boldsymbol{X}(k+1) = \boldsymbol{A}\boldsymbol{X}(k) + \boldsymbol{B}\boldsymbol{U}(k) + \boldsymbol{\Psi} \tag{6}$$

where $\boldsymbol{X} = (\boldsymbol{x}_1; ...; \boldsymbol{x}_N) \in \mathbb{R}^{3N\times 1}$, $\boldsymbol{U} = (\boldsymbol{u}_1, \dots, \boldsymbol{u}_N)^{\mathbf{T}}$, $\boldsymbol{A} = diag(A_1, \dots, A_N) \in \mathbb{R}^{3N\times 3N}$, $\boldsymbol{B} = diag(B_1, \dots, B_N) \in \mathbb{R}^{3N\times N}$, and $\boldsymbol{\Psi} = (\psi_1; \dots; \psi_N) \in \mathbb{R}^{3N\times N}$.

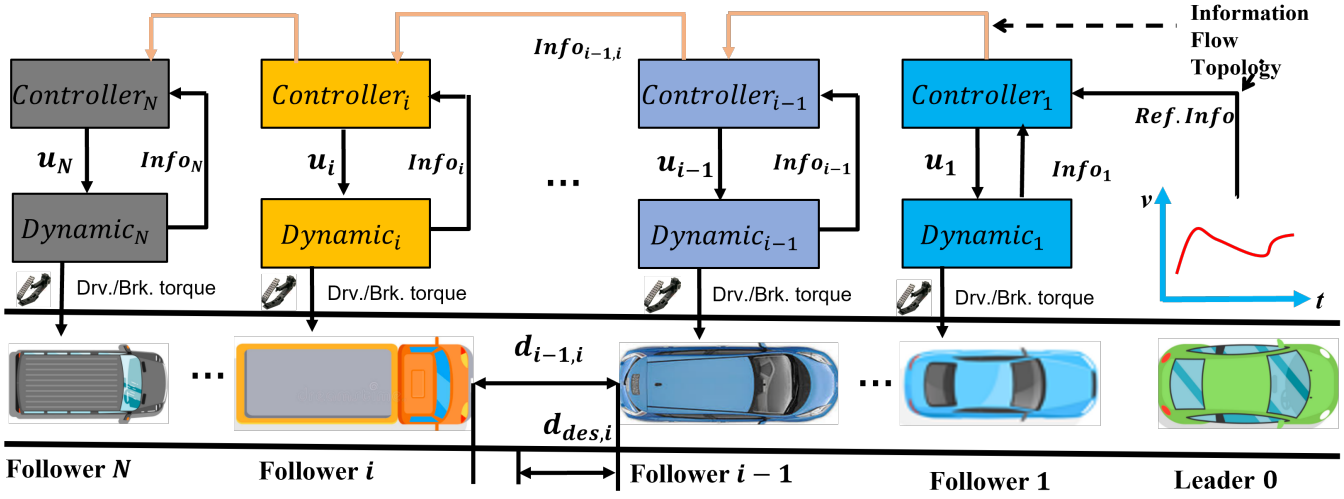

Fig. 1. Longitudinal heterogeneous platooning with information flow. Vehicles are controlled by their controllers, separately, to maintain safe and efficient platooning. Vehicles communicate according to the designed information topology.

B. Information Flow

The algebraic graph is utilized to describe information flow topology [39]. A Laplacian matrix and a pinning matrix are developed to describe the topology mathematically. The Laplacian matrix $\boldsymbol{L}$ depicts the communication directions among followers, which is defined as

$$\boldsymbol{L} = [l_{ij}] \in \mathbb{R}^{N\times N}, l_{ij} = \begin{cases} -\alpha_{ij}, & \text{if } j \neq i \\ \sum_{r=1,r\neq i}^{N} \alpha_{ir}, & \text{if } k = i \end{cases} \tag{7}$$

where $\alpha_{ij} = 1$ if the follower i receives information from follower j; otherwise, $\alpha_{ij} = 0$. The pinning matrix $\boldsymbol{P}$ represents the communication between the leader and followers, which is defined by

$$\boldsymbol{P} = \text{diag}\,(p_1, \ldots, p_N) \in \mathbb{R}^{N\times N} \tag{8}$$

where $p_i = 1$ if the follower i receives information from the leader; otherwise, $p_i = 0$. The above matrices vary according to different topologies. PF topology is used in this work.

C. The First-Order Second Moment (FOSM)

FOSM [37] is an approximation method to propagate the uncertainty from the input space to the output space. It is based on the performance function simplified by the first-order Taylor expansion. We denote the performance function by

$$Y = g(\boldsymbol{Z}) \tag{9}$$

where $\boldsymbol{Z} = (Z_1, \ldots, Z_n)^{\mathrm{T}}$ is a vector to represent input random variables, Y is the model response. Then, we linearize Eq. (9) by the first order Taylor expansion at the means of input random variables. The linearized performance function is given by

$$Y = g(\boldsymbol{Z}) \approx g\,(\boldsymbol{\mu_Z}) + \nabla g\,(\boldsymbol{\mu_Z}) \cdot (\boldsymbol{Z} - \boldsymbol{\mu_Z}) \tag{10}$$

where $\boldsymbol{\mu_Z}$ is a vector to represent the means of variables. The mean performance ($\boldsymbol{\mu}_Y$) is obtained by substituting $\boldsymbol{\mu_Z}$ into Eq. (10). The random variables in this study are assumed to be independent; therefore, the variance of the response $\boldsymbol{\sigma}_Y^2$ is given by

$$\boldsymbol{\sigma}_Y^2 = \sum_{l=1}^{n} \left(\frac{\partial g}{\partial Z_l}\right)^2 \Bigg|_{\boldsymbol{\mu_z}} \sigma_{Z_l}^2 \tag{11}$$

In this work, FOSM is used for uncertainty quantification of vehicle dynamics instead of sampling-based methods (e.g., Monte Carlo method) to reduce the computational cost.

D. Taguchi's Robustness

As shown in Fig. 2, Taguchi's robustness minimizes the effects of uncertainty in the design objective without eliminating the source of uncertainty. As a result, the design is insensitive to uncertainty. High robustness is obtained by changing the nominal values of design variables.

Using the notion of Taguchi's quality loss [30], we consider robustness in a broader sense: maximize the insensitivity of the response to uncertainty and their average performance. We now illustrate the idea using a nominal-the-best type performance. Let $\boldsymbol{T_r} = (T_{r1}, \ldots, T_{rm})^{\mathrm{T}}$ be the design targets, and the quality loss function is defined as

$$\mathcal{L}(\boldsymbol{Y}) = \sum_{i=1}^{m} w_i\,(Y_i - T_{ri})^2 \tag{12}$$

where w_i is a weighting factor determined by the cost. This quality loss consideration is the same as the loss function in MPC [17] and SMPC [23].

The quality loss $\mathcal{L}(\boldsymbol{Y})$ is a random variable. Taguchi's robustness is achieved by introducing another term in the traditional quality loss function. The modified loss function is given by

$$E_{\mathcal{L}(\boldsymbol{Y})} = \sum_{i=1}^{m} w_i \left[(\mu_{Y_i} - T_{ri})^2 + \sigma_{Y_i}^2\right] \tag{13}$$

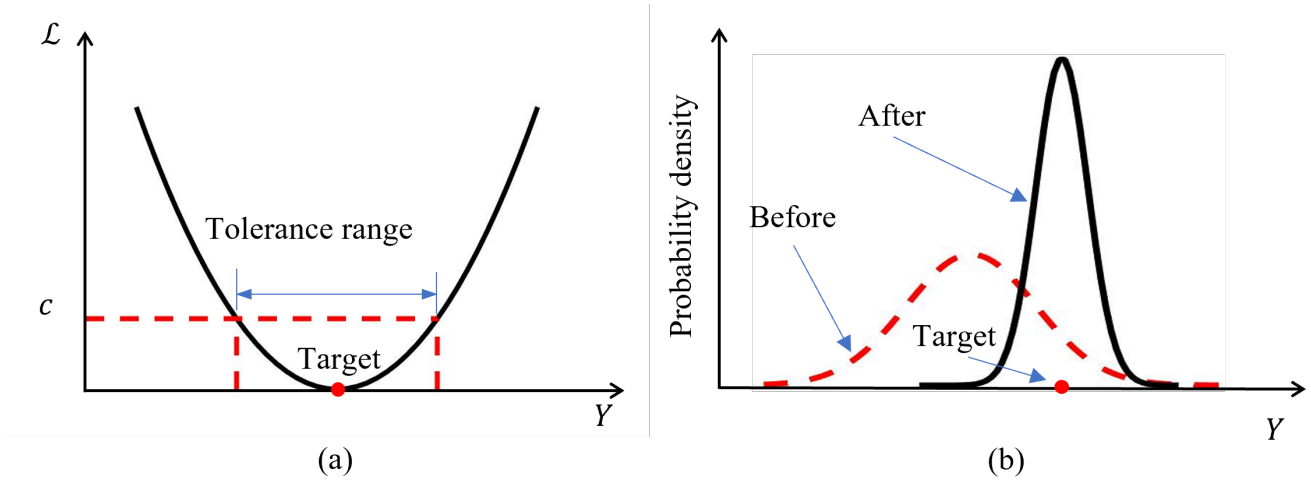

Fig. 2. The concept of Taguchi's robustness. (a) Quality loss function. (b) Robustness illustration. The robustness is achieved by balancing the mean target and its variation.

where $E_{\mathcal{L}(\boldsymbol{Y})}$ is the expected quality loss; μ_{Y_i} and $\sigma^2_{Y_i}$ are defined in Section II-C.

Minimizing Eq. (13) can bring the mean performance to the target and reduce the variation of the performance, which offers a balance between the mean performance and its variation. We modify the MPC cost function based on the idea to improve the controller performance under uncertainty.

III. Distributed SMPC with Taguchi's Robustness (TR-DSMPC)

The control objective is to enable the followers to track the leader with the desired gap between any adjacent vehicles. A constant spacing policy ($d_{i-1,i} = d_0$) is applied in this work, where d_0 is a predefined constant. The uncertainty considered in this work are from two parts, 1) vehicles: the mechanical efficiency coefficient (η_i) and inertial time lag (τ_i); 2) outside environment: aerodynamic drag coefficient (C_{a_i}) and rolling friction coefficient (f_i). PF topology is used to simulate the information flow as mentioned before. The uncertainty from vehicle communications is not considered in this work. Next, we introduce the methods for uncertainty modeling, the objective function formulation, and the constraints of optimization.

A. Uncertainty Modeling

The uncertainty of the parameters is considered in two ways in this work, time-independent and time-dependent uncertainty. Time-independent means that the parameter is constant over time. This simplified consideration is implemented in the current vehicle control design [16], [23]. However, the parameters are not always time-independent as studied in [40], [41]. For example, the friction factor changes along different locations of a road. The location or displacement is related to velocity and additionally to time. The vehicle state varies over time. Therefore, it is better to use time-dependent uncertainty.

Time-dependent uncertainties are modeled by stochastic processes. The values of the process at two time instants are correlated with respect to the distance (or time). The closer are the two points in a road, the stronger is their correlation. We employ stochastic processes (or called random fields) [42] to simulate the road condition related parameters, such as friction factor and air drag coefficient. The correlation between any arbitrary points t_1 and t_2 is described by an auto-correlation function (squared exponential kernel) that is defined by

$$\rho_{1,2} = \exp\left\{-\left(\frac{|t_1 - t_2|}{\theta_t}\right)^2\right\} \tag{14}$$

where θ_t is the correlation length along time.

In this work, we assume that the parameter uncertainties are Gaussian random fields. Then, the truncated Karhunen-Loeve (K-L) expansion [43] is utilized to generate the samples or functional data. The K-L expansion is given by

$$H(t) = \mu(t) + \sum_{i=1}^{M} \sqrt{\lambda_i}\varphi_i(t)\xi_i \tag{15}$$

where $\mu(t)$ is the mean function of the random field; λ_i and φ_i are the eigenvalues and eigen-functions of the auto-correlation function in Eq. (14); ξ_i is a group of independent standard normal variables; and M is the truncation number. When $\mu(t)$ is a constant that does not change with time, the random field is a stationary random field. In Section IV, we will provide two simulations that consider uncertainty as time-independent and time-dependent, respectively.

B. Objective Function

Similar to MPC, TR-DSMPC predicts the future behavior along a horizon (N_p) at each sampling time based on the current vehicle state. The optimal control signal is obtained by iteratively solving a local optimization problem in a sequence of time instances. With the availability of the current plant state $(\boldsymbol{X_p}(k) = (\boldsymbol{x}_{p,1}(k); \ldots; \boldsymbol{x}_{p,N}(k))^{\mathrm{T}} \in \mathbb{R}^{3N\times 1})$, we have the predicted control signal $(u_{p,i}(k+j+1))$ after local optimization, and the predictions along prediction horizon are obtained, which are denoted by $\boldsymbol{X_p}(k+j+1)$, where $j = 0, \ldots, N_{p-1}$.

Before introducing the objective function, we first define some terms which are used to formulate the optimization objective. The state of the leading vehicle is defined as $\boldsymbol{x}_0(t) = (s_0(t), v_0(t), T_0(t))^{\mathrm{T}}$ which is known. The desired state that the followers aim to track at instant k is denoted by $\boldsymbol{x}_{d,i}(k) = [s_{d,i}(k), v_{d,i}(k), T_{d,i}(k)]^{\mathrm{T}}$. And we have the desired control signal $u_{d,i}(k) = T_{d,i}(k)$. Then, the desired state for each follower is obtained by

$$\begin{cases} s_{d,i}(k) = s_0(k) - id_0 \\ v_{d,i}(k) = v_0(k) \\ T_{d,i}(k) = C_{a_i} v_0(k)^2 + m_i g f_i \end{cases} \tag{16}$$

Another term is the assumed state, $\boldsymbol{x}_{a,i}(k) = [s_{a,i}(k), v_{a,i}(k), T_{a,i}(k)]^{\mathrm{T}}$ which is obtained from the previous prediction of local optimization of the vehicle. The assumed state of vehicle i shifts along the time instances iteratively. The followers can not only track its assumed state but also treat the assumed state of other vehicles as the objective trajectory. In other words, all nodes can send information to node i, but the use of information from different nodes depends on the topology. Likewise, we have the assumed control signal $u_{a,i}(k)$.

For the PF topology used in this paper, the i-th vehicle only makes use of the information of $(i-1)$-th vehicle. We consider the control objective from three aspects that are safety, efficiency, and control, to optimize the spacing error of distance, the tracking error of speed, and the error of control signal. Therefore, the first part (similar to Eq. (12)) of the control objective of each following vehicle can be formulated as

$$\begin{aligned} E_{J_i}\left(\boldsymbol{y}_i(k), u_i(k)\right) = \sum_{j=0}^{N_p-1} \big(&\Delta \boldsymbol{y}_i^2(k+j+1) \\ &+ \Delta u_i^2(k+j+1) + \Delta \boldsymbol{y}_{a,i}^2(k+j+1) \end{aligned} \tag{17}$$

where $\boldsymbol{y}_i(k) = [s_i(k), v_i(k)]^{\mathrm{T}}$, hence $\Delta \boldsymbol{y}_i^2(k+j+1)$ and $\Delta y_{a,i}^2(k+j+1)$ represent the safety and efficiency, respectively; $\Delta u_i^2(k+j+1)$ represents the control error. We define $\beta = k+j+1$ and have

$$\Delta \boldsymbol{y}_i^2(\beta) = \left[\boldsymbol{y}_{p,i}(\beta) - \boldsymbol{y}_{d,i}(\beta)\right]^{\mathrm{T}} Q_{d,i} \left[\boldsymbol{y}_{p,i}(\beta) - \boldsymbol{y}_{d,i}(\beta)\right] \tag{18}$$

$$\begin{aligned} \Delta \boldsymbol{y}_{a,i}^2(\beta) = &\left[\boldsymbol{y}_{p,i}(\beta) - \boldsymbol{y}_{a,i}(\beta)\right]^{\mathrm{T}} W_{a,i} \left[\boldsymbol{y}_{p,i}(\beta) - \boldsymbol{y}_{a,i}(\beta)\right] \\ &+ \left[\boldsymbol{y}_{p,i}(\beta) - \boldsymbol{y}_{a,i-1}(\beta)\right]^{\mathrm{T}} W_{n,i} \left[\boldsymbol{y}_{p,i}(\beta) - \boldsymbol{y}_{a,i-1}(\beta)\right] \end{aligned} \tag{19}$$

$$\Delta u_i^2(\beta) = \left[u_{p,i}(\beta) - u_{a,i}(\beta)\right]^T R_i \left[u_{p,i}(\beta) - u_{a,i}(\beta)\right] \tag{20}$$

where $Q_{d,i} \in \mathbb{R}^{2\times 2}$, $W_{a,i} \in \mathbb{R}^{2\times 2}$, $W_{n,i} \in \mathbb{R}^{2\times 2}$, $R_i \in \mathbb{R}^{1\times 1}$ are weighting matrices or weighting factors.

Next, we derive the second part of the objective function, the variance of $\Delta \boldsymbol{y_i}$, $\Delta \boldsymbol{y}_{a,i}$, and Δu_i denoted by $\sigma_{\Delta y_i}^2$, $\sigma_{\Delta y_{a,i}}^2$, and $\sigma_{\Delta u_i}^2$, respectively, where $\Delta \boldsymbol{y_i} = \left[\boldsymbol{y}_{p,i}(\beta) - \boldsymbol{y}_{d,i}(\beta)\right]^{\mathrm{T}}$, $\Delta \boldsymbol{y}_{a,i} = \left[\boldsymbol{y}_{p,i}(\beta) - \boldsymbol{y}_{a,i}(\beta)\right]^T + \left[\boldsymbol{y}_{p,i}(\beta) - \boldsymbol{y}_{a,i-1}(\beta)\right]^{\mathrm{T}}$, and $\Delta u_i = \left[u_{p,i}(\beta) - u_{a,i}(\beta)\right]^{\mathrm{T}}$.

As mentioned in Section II-A, η_i, C_{a_i}, f_i, and τ_i are uncertain parameters. According to Eq. (9), we have $\boldsymbol{Z}_i = [Z_{i,1}, Z_{i,2}, Z_{i,3}, Z_{i,4}]^{\mathrm{T}} = [\eta_i, C_{a_i}, f_i, \tau_i]^{\mathrm{T}}$. We simplify Eq. (1) as

$$\begin{aligned} \boldsymbol{y}_i(t) &= \left[s_i\left(\boldsymbol{Z}_i, t\right), v_i\left(\boldsymbol{Z}_i, t\right)\right] = f\left(\boldsymbol{Z}_i, t\right) \\ &= f\left(\eta_i, C_{a_i}, f_i, \tau_i, t\right) \end{aligned} \tag{21}$$

Since $\boldsymbol{y}_{d,i}(\beta)$, $\boldsymbol{y}_{a,i}(\beta)$, $\boldsymbol{y}_{a,i-1}(\beta)$ are constant, according to Eq. (11), we have the standard deviation $\sigma_{\Delta \boldsymbol{y}_i}(k)$ at the k-th instance which is obtained by

$$\begin{aligned} \sigma_{\Delta \boldsymbol{y}_i}(k) &= \left[\sigma_{\Delta s_i}, \sigma_{\Delta v_i}\right]^{\mathrm{T}} \\ &= \left[\sqrt{\sum_{l=1}^{4} \left(\frac{\partial s_i\left(\boldsymbol{Z}_i, k\right)}{\partial Z_{i,l}}\right)^2 \sigma_{Z_l}^2}, \sqrt{\sum_{l=1}^{4} \left(\frac{\partial v_i\left(\boldsymbol{Z}_i, k\right)}{\partial Z_{i,l}}\right)^2 \sigma_{Z_l}^2}\right]^{\mathrm{T}} \end{aligned} \tag{22}$$

The variance ($\sigma_{\Delta \boldsymbol{y}_i}^2(k)$) is obtained by

$$\sigma_{\Delta \boldsymbol{y}_i}^2(k) = \left[\sigma_{\Delta s_i}, \sigma_{\Delta v_i}\right] Q_{d,i} \left[\sigma_{\Delta s_i}, \sigma_{\Delta v_i}\right]^{\mathrm{T}} \tag{23}$$

Similarly, we have

$$\begin{aligned} \sigma_{\Delta \boldsymbol{y}_{a,i}}^2(k) = &\left[\sigma_{\Delta s_i}, \sigma_{\Delta v_i}\right] W_{a,i} \left[\sigma_{\Delta s_i}, \sigma_{\Delta v_i}\right]^{\mathrm{T}} \\ &+ \left[\sigma_{\Delta s_i}, \sigma_{\Delta v_i}\right] W_{n,i} \left[\sigma_{\Delta s_i}, \sigma_{\Delta v_i}\right]^{\mathrm{T}} \end{aligned} \tag{24}$$

According to Eq. (16) that $u_{d,i}(k) = T_{d,i}(k) = C_{a_i} v_0(k)^2 + m_i g f_i$ and Eq. (20), we have

$$\sigma_{\Delta \boldsymbol{u}_i}^2(k) = R_i \sigma_{\Delta \boldsymbol{u}_i}^2(k) \tag{25}$$

The variation term in Eq. (13) is given by

$$\begin{aligned} V_{J_i}\left(\boldsymbol{y}_i(k), u_i(k)\right) = \sum_{j=0}^{N_p-1} \Big[&w_{\Delta \boldsymbol{y}_i} \sigma_{\Delta \boldsymbol{y}_i}^2(k+j+1) \\ &+ w_{\Delta \boldsymbol{y}_{a,i}} \sigma_{\Delta \boldsymbol{y}_{a,i}}^2(k+j+1) + \sigma_{\Delta \boldsymbol{u}_i}^2(k+j+1)\Big] \end{aligned} \tag{26}$$

where $w_{\Delta \boldsymbol{y}_i}$ and $w_{\Delta \boldsymbol{y}_{a,i}}$ are the weighting factors for $\sigma_{\Delta \boldsymbol{y}_i}^2$ and $\sigma_{\Delta \boldsymbol{y}_{a,i}}^2$, respectively. Because $\sigma_{\Delta \boldsymbol{u}_i}^2$ is far larger than $\sigma_{\Delta \boldsymbol{y}_i}^2$ and $\sigma_{\Delta \boldsymbol{y}_{a,i}}^2$, weighting factors need to be applied to show the influence of the two terms in optimization.

In summary, the weighted optimization objective is formulated as

$$J_i\left(\boldsymbol{y}_i(k), u_i(k)\right) = E_{J_i}\left(\boldsymbol{y}_i(k), u_i(k)\right) + V_{J_i}\left(\boldsymbol{y}_i(k), u_i(k)\right) \tag{27}$$

C. Constraints

The constraints include control signal bounds, vehicle dynamics constraints, and probabilistic constraints (chance constraints). The control signal bounds indicate the limitation of control inputs. The vehicle dynamics constraints are the equality constraints to ensure that vehicle dynamics is physically feasible. And the probabilistic constraints or reliability constraints are applied to the terminal state of local optimization to ensure that vehicles operate within the vicinity of a predefined safety region.

TABLE I
INFORMATION OF DETERMINISTIC PARAMETERS AND RANDOM PARAMETERS

Random Variables	Distribution	Mean	Standard deviation
$m_{1,\ldots,7}$ (kg)	Deterministic	(2.5, 2.3, 2.0, 1.9, 1.7, 1.6, 1.5)$\times 10^3$	-
$R_{1,\ldots,7}$ (m)	Deterministic	(0.45, 0.45, 0.3, 0.3, 0.27, 0.24, 0.23)	-
$\eta_{1,\ldots,7}$	Uniform	0.92	0.0346
$C_{A,1,\ldots,7}(\mathrm{N}\cdot\mathrm{s}^2\mathrm{m}^{-2})$	Normal	(0.9, 0.9, 0.7, 0.7, 0.45, 0.45, 0.45)	(0.135, 0.135, 0.105, 0.105, 0.0675, 0.0675, 0.0675)
$\tau_{1,\ldots,7}(\mathrm{s})$	Uniform	0.5	0.1732
$f_{1,\ldots,7}$	Normal	0.01	0.001

For i-th vehicle, the bounded constraints and dynamics constraints are denoted by

$$\begin{cases} u_{lb,i}(k+j+1) < u_{p,i}(k+j+1) < u_{ub,i}(k+j+1) \\ \dot{\boldsymbol{x}}_i(j+1) = A_i \boldsymbol{x}_i(j) + B_i u_i(j) + C_i \\ j = 0, 1, \ldots, N_p - 1 \end{cases} \tag{28}$$

The probabilistic constraints of the terminal state are based on the standard deviation of spacing error ($\sigma_{\Delta s_i}$), relative velocity ($\sigma_{\Delta v_i}$), and control error ($\sigma_{\Delta u_i}(k)$). By multiplying the standard deviation by a scaling factor δ, the probabilistic constraints are shown below.

$$\begin{cases} -\delta\sigma_{\Delta s_i} < s_i\left(k+N_p\right) - s_{d,i}\left(k+N_p\right) < \delta\sigma_{\Delta s_i} \\ -\delta\sigma_{\Delta v_i} < v_i\left(k+N_p\right) - v_{d,i}\left(k+N_p\right) < \delta\sigma_{\Delta v_i} \\ -\delta\sigma_{\Delta u_i} < T_i\left(k+N_p\right) - T_{d,i}\left(k+N_p\right) < \delta\sigma_{\Delta u_i} \end{cases} \tag{29}$$

which means that the spacing error, relative velocity, and control error are within the 2δ standard deviation of the desired state.

D. Optimization Formulation

With the objective function and constraints discussed above, we have the proposed optimization model for each vehicle as follows:

$$\begin{aligned} \min_{\boldsymbol{U}_i} \quad & J_i\left(\boldsymbol{y}_i(k), u_i(k)\right) \\ \text{s.t.} \quad & u_{lb,i}(k+j+1) < u_{p,i}(k+j+1) < u_{ub,i}(k+j+1) \\ & \dot{\boldsymbol{x}}_i(j+1) = A_i \boldsymbol{x}_i(j) + B_i u_i(j) + C_i \\ & -\delta\sigma_{\Delta s_i} < s_i\left(k+N_p\right) - s_{d,i}\left(k+N_p\right) < \delta\sigma_{\Delta s_i} \\ & -\delta\sigma_{\Delta v_i} < v_i\left(k+N_p\right) - v_{d,i}\left(k+N_p\right) < \delta\sigma_{\Delta v_i} \\ & -\delta\sigma_{\Delta u_i} < T_i\left(k+N_p\right) - T_{d,i}\left(k+N_p\right) < \delta\sigma_{\Delta u_i} \\ & j = 0, 1, \ldots, N_p - 1 \end{aligned} \tag{30}$$

In summary, the proposed method (TR-DSMPC) can be viewed as an extension of SMPC. Different from SMPC, TR-DSMPC incorporates Taguchi's robustness in the control objective that maximizes the mean performance and minimizes its variations. The robustness of the proposed method is to maximize the mean performance and minimize the variation of the performance, which is different from the robustness of RMPC that minimizes the worst case. Besides, TR-DSMPC employs an approximation uncertainty quantification method (FOSM), which is far more efficient than Monte Carlo based sampling methods that classical SMPC employs. Next, we use two simulations to illustrate the control effect of TR-DSMPC.

IV. NUMERICAL SIMULATION

In this section, we provide two simulations to evaluate the performance of TR-DSMPC. Both two simulations contain one leading vehicle (numbered by 0) and seven followers (numbered from 1 to 7) under PF topology. The desired space (d_0) between any two adjacent vehicles is 20 m. In other words, the distance from the rear end of the preceding vehicle to the front end of the following vehicle is designed to be 20 m. The detailed settings of the two simulations are as follows.

- The whole simulation time is 48 s with the simulation time step of 0.2 s;
- The leading vehicle starts with an initial speed of 25 m/s, and it decelerates from 3 to 5 s with -4 m/s^2 and accelerate from 27 to 35 s with 1 m/s^2;
- The initial velocity of all followers is 30 m/s, and the initial spacing error between any adjacent vehicles are 0 m;
- The maximum and minimum acceleration for all followers are 1.5 m/s^2 and -8 m/s^2, respectively.

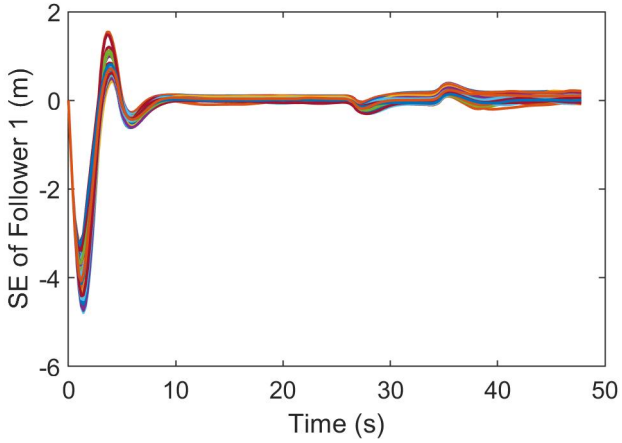

Fig. 3. An illustration of performance variation under uncertainty. It includes random spacing errors of Follower 1 from 100 simulations with 100 samples of random parameters. It shows the variation of controller performance due to uncertainty.

Using the same scenario, we compare TR-DSMPC with nominal distributed nominal MPC (DMPC) and distributed stochastic MPC (DSMPC) for the two simulations. A prediction horizon length (N_p) needs to be determined for all of the three methods. It is revealed that the computational cost increases with the increasing of prediction horizon [44], [45]. For TR-DSMPC and DSMPC, we found that $N_p = 10$ is good enough to fulfill the control objective. However, DMPC

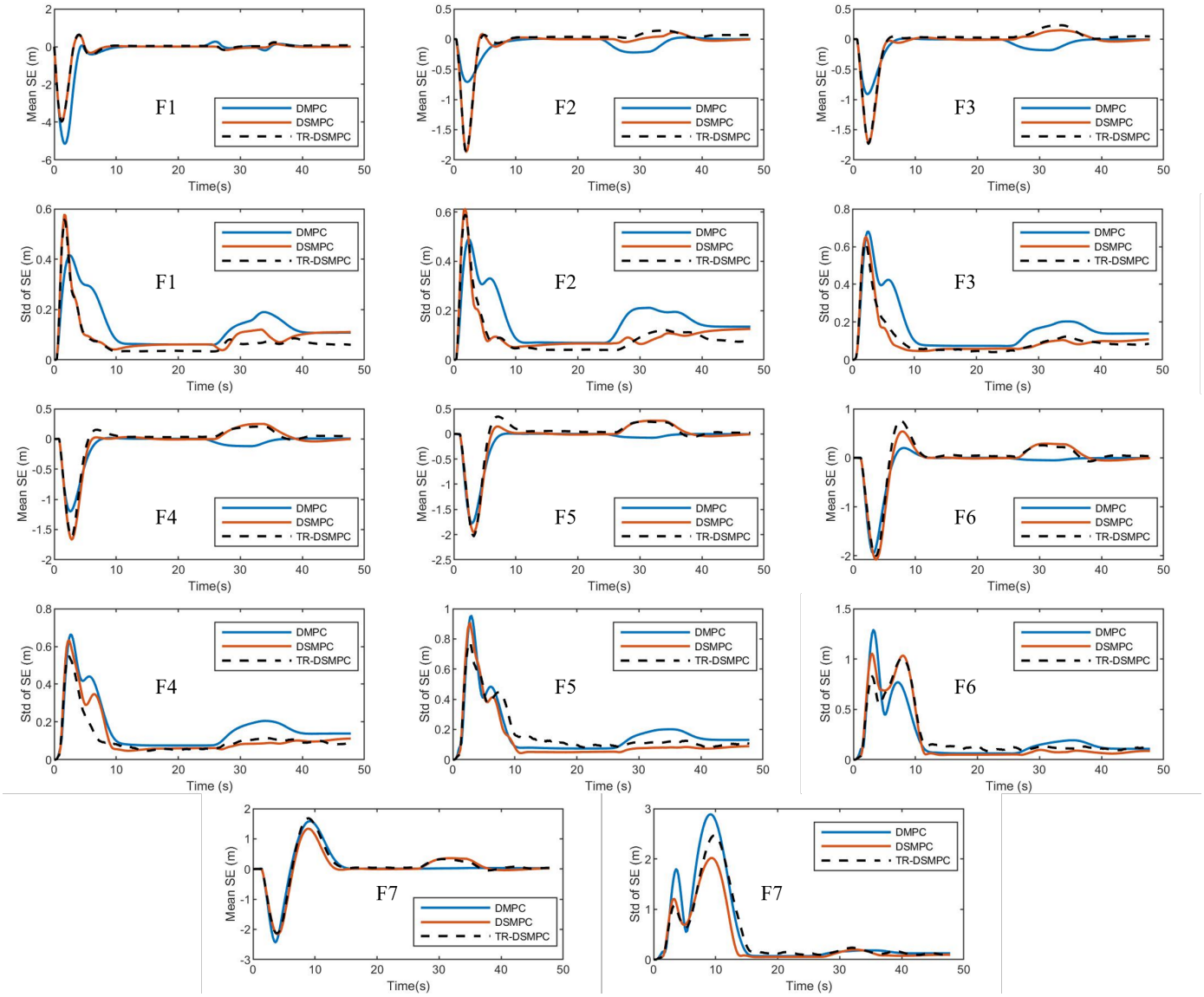

Fig. 4. Means and standard deviations of spacing errors of followers with random variables. SE - spacing error; Std - standard deviation; F1–F7: Followers 1 to 7. The results are obtained from 100 control simulations.

needs a minimum prediction horizon of 20; namely, $N_p = 20$. Hence, we use $N_p = 10$ for TR-DSMPC and DSMPC and $N_p = 20$ for DMPC.

Due to the randomness of the model parameters, we execute the control task using Monte Carlo Simulation (MCS) with a sample size of 100 to assess the performance of different methods. As mentioned in Section II-A, the random parameters include the mechanical efficiency coefficient (η_i), aerodynamic drag coefficient (C_{a_i}), rolling friction coefficient (f_i), and inertial time lag (τ_i). Their distributions and other model parameters are provided in Table I.

Next, we discuss the details of the two simulations and the results.

A. Time-independent randomness

In this simulation, we treat the uncertainty as time-independent, which means that the parameters are constant over time. The 100 MCS samples are randomly generated from the distributions of the parameters. The randomness of the parameters is propagated to the vehicle state (position, velocity, and torque), which leads to performance fluctuation of the controllers.

We evaluate the controller performance from two aspects, safety (spacing error) and efficiency (relative velocity). The spacing error (SE) of Follower 1 is presented in Fig. 3 from the 100 MCS samples. It is shown that the spacing error curves vary with different values of the uncertain parameters. The different values represent different road conditions during the platooning task. We obtain similar results of relative velocity (RV) for other followers using other control methods (DMPC, DSMPC). To better show the difference of the methods, we provide the statistical properties (mean and standard deviation) in terms of SE and RV along time to assess the performance of different methods.

TABLE II
MAXIMUM AND AVERAGE OF STATISTICAL PERFORMANCE FOR SIMULATION 1.

Follower	Methods	Spacing Error (m)				Relative velocity (m/s)			
		Mean		Std		Mean		Std	
		Average	Max	Average	Max	Average	Max	Average	Max
1	DMPC	0.3169	5.1453	0.1308	0.4150	0.3144	5.0	0.0407	0.3439
	DSMPC	0.2079	3.9658	0.0974	0.5767	0.2583	5.0	0.0477	0.7088
	TR-DSMPC	0.2377	**3.9751**	**0.0752**	0.5569	**0.2647**	5.0	**0.0453**	0.6772
2	DMPC	0.0939	0.7094	0.1565	0.4906	0.0401	0.6917	0.0510	0.4443
	DSMPC	0.1029	1.8674	0.1044	0.6129	0.0956	1.6206	0.0546	0.7764
	TR-DSMPC	0.1268	1.8731	**0.0944**	0.5892	0.0908	1.6499	0.0571	0.7295
3	DMPC	0.0923	0.9107	0.1692	0.6793	0.0460	0.9119	0.0618	0.6169
	DSMPC	0.1237	1.7087	0.1039	0.6524	0.0818	1.2571	0.0594	0.7826
	TR-DSMPC	0.1408	1.7355	**0.1036**	**0.6214**	0.0845	1.2375	0.0676	0.7483
4	DMPC	0.1021	1.2009	0.1671	0.6630	0.0560	1.0958	0.0626	0.6491
	DSMPC	0.1450	1.6670	0.1209	0.6321	0.0843	1.2023	0.0742	0.7518
	TR-DSMPC	0.1485	1.6258	**0.1076**	**0.5475**	0.0841	1.1727	0.0834	0.6919
5	DMPC	0.1285	1.7713	0.1774	0.9524	0.0774	1.3873	0.0801	0.9038
	DSMPC	0.1734	1.9551	0.1311	0.9066	0.1010	1.2388	0.0962	0.9177
	TR-DSMPC	0.1946	2.0354	0.1695	**0.7766**	0.1133	1.2833	0.1344	**0.8586**
6	DMPC	0.1379	1.9507	0.2111	1.2898	0.0919	1.4281	0.120	1.1396
	DSMPC	0.2158	2.0790	0.2004	1.0535	0.1242	1.1925	0.1353	0.9804
	TR-DSMPC	0.2239	2.0034	0.2303	**1.0119**	0.1327	1.1884	0.1788	**0.9050**
7	DMPC	0.3028	2.4295	0.5128	2.8870	0.1685	1.5240	0.2452	1.4290
	DSMPC	0.3057	2.1530	0.3575	2.0190	0.1641	1.2230	0.2047	1.0563
	TR-DSMPC	0.3472	**2.1306**	0.4639	2.4693	0.1786	1.2504	0.2723	**0.9294**

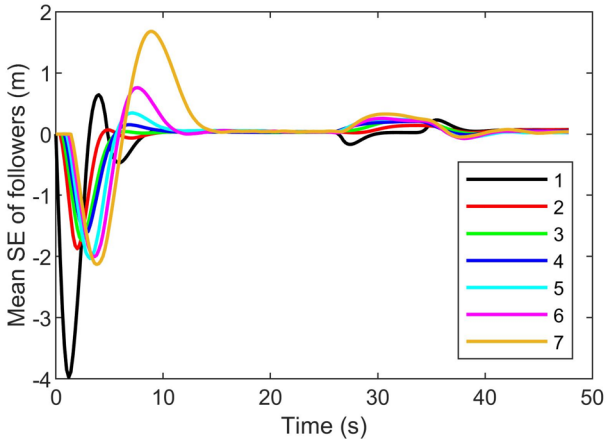

Fig. 5. Mean spacing error tracking of seven followers under time-independent randomness assumption.

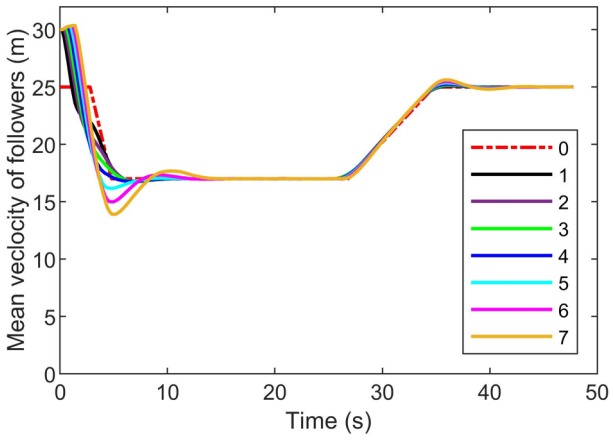

Fig. 6. Mean velocity tracking of seven followers under time-independent randomness assumption.

The spacing errors of seven followers are shown in Fig. 4. DMPC has a good performance on the mean spacing error, but its standard deviation is larger than DSMPC in general, especially for Follower 7. TR-DSMPC has a similar mean performance in spacing error with DSMPC with smaller variation than DSMPC, except for Follower 7. We have similar results for relative velocity which are not provided in the paper for space consideration. To better show the difference of different methods, we provide the maximum value of mean and standard deviation of spacing error, average value of mean and standard deviation of spacing error, maximum value of mean and standard deviation of relative velocity, average value of mean and standard deviation of relative velocity in Table II.

The bold numbers represent the better performance of the proposed method compared with other methods. According to Table II, Follower 1 has improvement in both safety and efficiency. Both the average of standard deviations for spacing error and relative velocity are decreased, especially for the spacing error (0.0752), although the average of mean spacing error increases to 0.2377 compared with DSMPC. TR-DSMPC for Followers 2–4 has a smaller average value for the standard deviation of spacing error compared with other methods. And only the maximum values either for spacing error or relative velocity are smaller than other methods for Followers 5–7. Overall, TR-DSMPC for Follower 1 has the most significant improvement.

The tracking performance of TR-DSMPC in terms of mean spacing error and mean velocity of all followers are provided

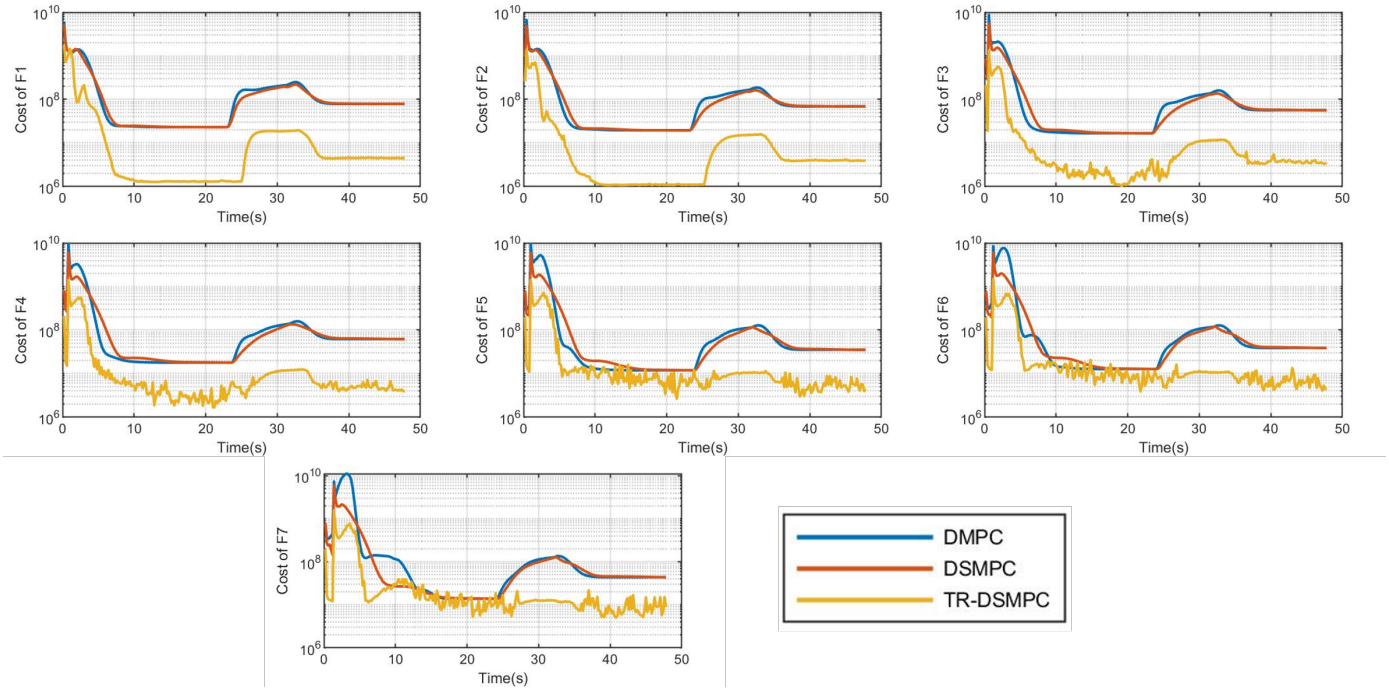

Fig. 7. The optimization objective (cost) over time for different methods under time-independent randomness assumption. The loss of all methods are from two parts, the mean performance and its variance.

TABLE III
MEAN COST AT TWO TIME PERIODS FOR SIMULATION 1

Follower	Mean cost ($\times 10^7$)					
	15–27 s			38–48 s		
	DMPC	DSMPC	TR-DSMPC	DMPC	DSMPC	TR-DSMPC
1	5.547	4.421	**0.251**	7.911	7.939	**0.450**
2	3.816	2.915	**0.155**	6.926	6.953	**0.396**
3	2.960	2.254	**0.213**	5.676	5.738	**0.369**
4	2.783	2.277	**0.345**	6.210	6.330	**0.484**
5	1.906	1.589	**0.699**	3.540	3.616	**0.530**
6	1.830	1.651	**0.887**	3.904	4.0	**0.612**
7	1.876	1.743	**1.130**	4.381	4.513	**0.858**

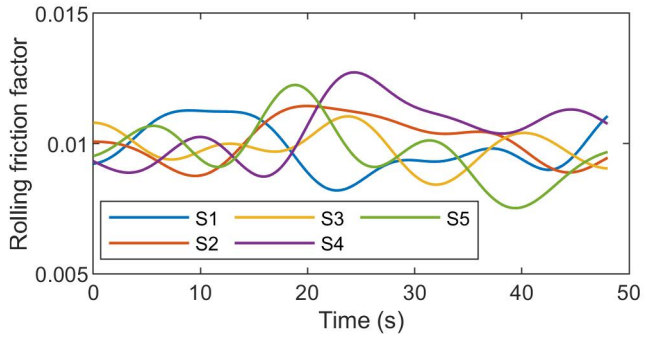

Fig. 8. An example of time-dependent randomness. The figure shows five possibilities that the rolling friction factor varies at different locations on a road.

in Figs. 5 and 6. It is shown that all followers can successfully track the behavior of the leading vehicle by maintaining ideal spacing and velocity upon steady state from around 15–27 s and 38–48 s.

Except for the mean spacing error, we also provide the mean cost of the optimization objective for different methods in Fig. 7. DMPC and DSMPC only minimize the cost of mean performance. TR-DSMPC minimizes the cost of both the mean performance and its variation. After the control optimization is finished, we add the cost induced by the their variations to the objective of DMPC and DSMPC, so that we compare the cost for different methods using the same scale. From Fig. 7, TR-DSMPC has the best performance by minimizing the cost of mean performance and its variation for all vehicles. As mentioned previously, the vehicles are in steady state from 15–27 s and 38–48 s. We compare the average of the mean cost quantitatively for the two time periods in Table III. The cost for TR-DSMPC decreases significantly at the two steady periods.

B. Time-dependent randomness

In the second simulation, we consider more realistic uncertainties, the time-dependent uncertainty. Specifically, aerodynamic drag coefficient (C_{a_i}) and rolling friction coefficient (f_i) are modeled by stochastic processes. The other two parameters are still random variables. The stochastic processes are used to generate samples with the squared exponential kernel function as discussed in Section III-A. We set the term $\mu(t)$ in Eq. (15) as a constant so that the stochastic processes are stationary. The generated five samples for f_i are shown in Fig. 8.

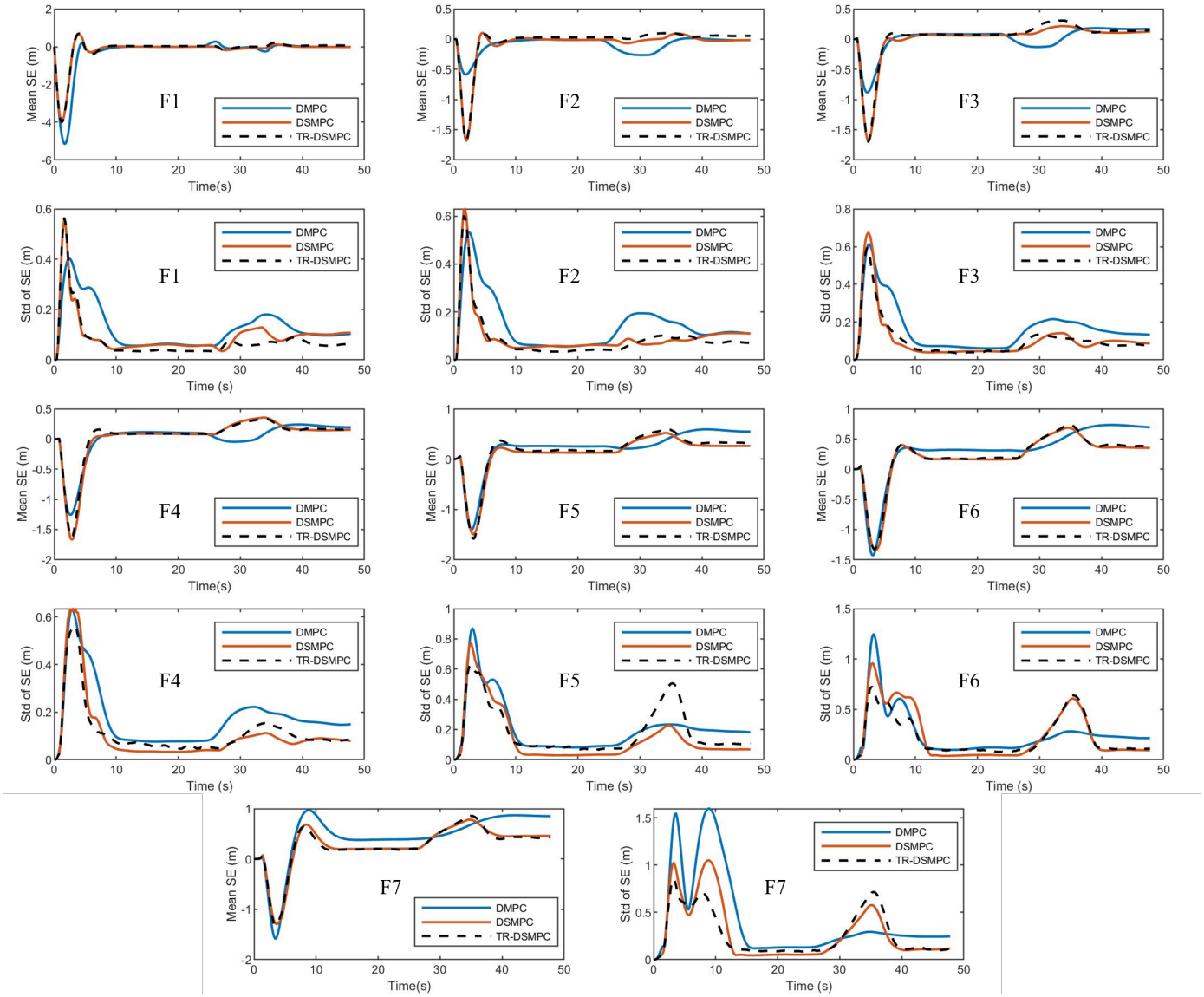

Fig. 9. Means and standard deviations of spacing errors of followers with random process. The results are obtained based on 100 control simulations.

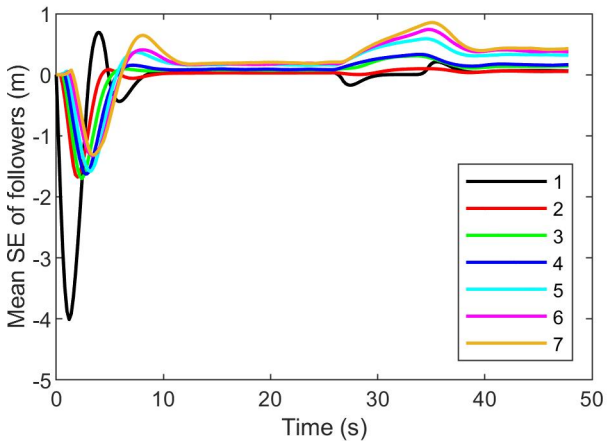

Fig. 10. Mean spacing error tracking of seven followers under time-dependent randomness assumption.

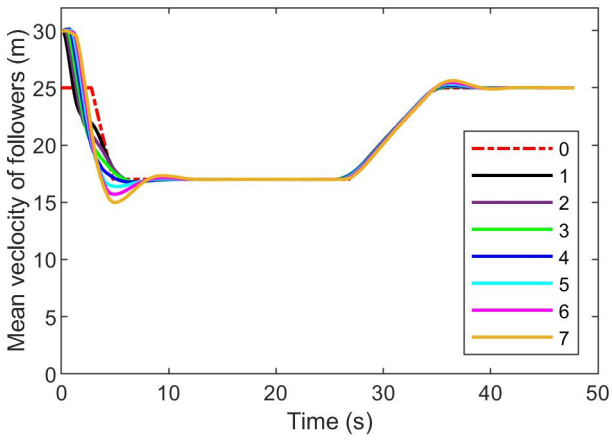

Fig. 11. Mean velocity tracking of seven followers under time-dependent randomness assumption.

TABLE IV
MAXIMUM AND AVERAGE OF STATISTICAL PERFORMANCE FOR SIMULATION 2

Follower	Methods	Spacing Error (m)				Relative velocity (m/s)			
		Mean		Std		Mean		Std	
		Average	Max	Average	Max	Average	Max	Average	Max
1	DMPC	0.3109	5.1444	0.1252	0.4028	0.3165	5.0002	0.0474	0.3435
	DSMPC	0.210	3.9979	0.0948	0.5576	0.2597	5.0002	0.0545	0.7024
	TR-DSMPC	0.2330	**4.0115**	**0.0759**	0.5629	**0.2669**	5.0002	**0.0507**	0.7227
2	DMPC	0.0927	0.5862	0.1434	0.5330	0.0364	0.6570	0.0565	0.4739
	DSMPC	0.0966	1.6836	0.0959	0.6303	0.0879	1.4395	0.0590	0.7928
	TR-DSMPC	0.1088	1.6778	**0.0871**	0.6002	0.0814	1.4684	**0.0580**	0.7651
3	DMPC	0.1449	0.8857	0.1652	0.6127	0.0508	0.8939	0.0645	0.5654
	DSMPC	0.1686	1.6943	0.1057	0.6747	0.0806	1.3382	0.0672	0.7490
	TR-DSMPC	0.1946	1.7005	**0.1047**	**0.5931**	0.0848	1.2920	0.0690	0.6890
4	DMPC	0.1845	1.2599	0.1752	0.6308	0.0653	1.1295	0.0684	0.5564
	DSMPC	0.2249	1.6680	0.1059	0.6346	0.0824	1.1845	0.0716	0.6291
	TR-DSMPC	**0.2189**	1.6307	0.1134	**0.5631**	0.0850	**1.1310**	0.0838	**0.5931**
5	DMPC	0.3820	1.4002	0.2082	0.8695	0.0779	1.1974	0.0906	0.8018
	DSMPC	0.2959	1.4944	0.1402	0.7705	0.0854	1.0812	0.0969	0.7727
	TR-DSMPC	**0.3430**	1.5849	**0.1861**	**0.6276**	0.0980	1.0924	0.1234	**0.6863**
6	DMPC	0.4701	1.4258	0.2546	1.2467	0.0790	1.0971	0.1152	1.0965
	DSMPC	0.3642	1.3454	0.2458	0.9578	0.0897	0.9172	0.1394	0.8675
	TR-DSMPC	**0.3742**	**1.3320**	**0.2281**	**0.7248**	0.0941	0.9164	0.1503	**0.6850**
7	DMPC	0.6082	1.5853	0.4179	1.5976	0.1107	1.1159	0.1865	1.2410
	DSMPC	0.4281	1.2951	0.2773	1.0506	0.1011	0.8784	0.1604	0.8722
	TR-DSMPC	**0.4129**	**1.3132**	**0.2678**	**0.8514**	0.1082	0.9699	0.1708	0.7499

TABLE V
MEAN COST AT TWO TIME PERIODS FOR SIMULATION 2.

Follower	Mean cost ($\times 10^7$)					
	15–27 s			38–48 s		
	DMPC	DSMPC	TR-DSMPC	DMPC	DSMPC	TR-DSMPC
1	5.570	4.458	**0.253**	7.902	7.925	**0.448**
2	3.864	2.954	**0.158**	6.920	6.952	**0.393**
3	2.954	2.340	**0.228**	5.973	6.018	**0.421**
4	2.690	2.393	**0.278**	6.709	6.668	**0.498**
5	2.068	1.971	**0.504**	5.720	5.033	**0.610**
6	2.539	2.351	**0.536**	9.167	7.225	**0.839**
7	3.490	2.927	**0.725**	14.045	10.175	**1.316**

Similarly, the mean spacing errors and their standard deviations are provided in Fig. 9. The uncertainty consideration is more complex than the previous simulation. The mean spacing errors of DMPC increase from Followers 1 to 7 after convergence. The standard deviations of DMPC are larger than TR-DSMPC and DSMPC in general. TR-DSMPC has a similar mean performance to DSMPC. The variations of spacing error for Followers 1–3 decrease, however, the differences from the figure for Followers 4–7 are subtle. Similarly, the figure for relative velocity is voided for space consideration.

Likewise, Table IV is provided to show the subtle difference between different methods. Overall, Follower 1 has the most significant improvement by TR-DSMPC. TR-DSMPC has the lowest average standard deviation of spacing error (0.0759) that decreased around 20% compared with DSMPC, and its average value of mean spacing error only increases a bit. The average value of mean relative velocity is smaller than DMPC but slightly larger than DSMPC, and the average value of its standard deviation is smaller than DSMPC but larger than DMPC. Spacing error and relative velocity represent the safety and efficiency of platooning, respectively. Therefore, we see that Follower 2 has improvement in both safety and efficiency, specifically, lower average standard deviation than other methods. As for Followers 3–7, the main improvement is in safety with either smaller average values of the mean spacing error or smaller average values of its standard deviation.

The tracking performance (mean spacing error and mean velocity) of TR-DSMPC for all followers is shown in Figs. 10 and 11. The mean spacing errors are with small errors for Followers 4–7 after convergence, because of the complex uncertainty consideration. All followers can track the speed of the leading vehicle well.

The mean cost for different methods in this simulation has the similar pattern to the cost in the previous one. We avoid the cost figure for the example. A mean cost table (Table V) at the two steady periods is given below. TR-DSMPC still outperforms DMPC and DSMPC for the more complex uncertainty consideration.

TABLE VI
COMPARISON OF THE COMPUTATIONAL COST OF DIFFERENT METHODS FOR TWO SIMULATIONS.

Simulation	Method	Computation time (s)
Time-independent randomness	DMPC	118.59
	DSMPC	206.55
	TR-DSMPC	403.66
Time-dependent randomness	DMPC	118.59
	DSMPC	206.55
	TR-DSMPC	403.66

For a fair comparison, we also provide the computational complexity of different methods in terms of computation time for both simulations in Table VI. The proposed method needs more computational time due to a more complex objective function.

Moreover, we tested two additional cases with the two

uncertainty modeling methods. One includes four followers with random initial spacing errors, and the other includes 10 followers with both random initial spacing errors and random initial velocities. Therefore, we have four additional simulations in total. The simulation results are consistent with the results above.

V. Conclusions

In this paper, we proposed a new control methodology (TR-DSMPC) for longitudinal heterogeneous vehicle platooning by introducing Taguchi's robustness into distributed stochastic model predictive control. The first order second moment (FOSM) was used for uncertainty quantification, which is far more efficient than Monte Carlo-based methods. The simulation results showed that TR-DSMPC can successfully reduce the performance variations by maintaining the mean performance. The cost comparison between different methods showed that the robustness is improved by minimizing the mean performance and its variation. The reason that the improvement is not significant for some vehicles can be explained follows:

- The PF topology may not be perfect for this platooning task. The evidence is as follows: 1) Follower 1 that receives information from the leading vehicle has a significant improvement, and 2) Other followers that do not receive information from the leading vehicle have a much smaller improvement.
- Robust design has a better performance for nonlinear models than linear models. The performance could be significantly improved if a model has a higher nonlinearity.

Reliability consideration in this work is to force vehicles operating within a pre-defined range centered at the target state. The range size depends on uncertainty of the vehicle state. We can also use a threshold of spacing error or other criteria to determine the vehicle is safe or not. The state variables are assumed to be independent.

One future research direction is to study the influence of different information flow topology on control performance. It is also interesting to investigate the performance of TR-DSMPC for more complex application scenarios (e.g. platooning with both longitudinal and lateral motions). At last, the uncertainty from vehicle communications and the dependency between state variables can be considered and incorporated into our proposed approach.

Acknowledgments

The authors would like to acknowledge the support from the IUPUI Institute of Integrated Artificial Intelligence (iAI) and the National Science Foundation under Grant No 1923799.

References

[1] B. Van Arem, C. J. Van Driel, and R. Visser, "The impact of cooperative adaptive cruise control on traffic-flow characteristics," *IEEE Transactions on Intelligent Transportation Systems*, vol. 7, no. 4, pp. 429–436, 2006.

[2] K. C. Dey, L. Yan, X. Wang, Y. Wang, H. Shen, M. Chowdhury, L. Yu, C. Qiu, and V. Soundararaj, "A review of communication, driver characteristics, and controls aspects of cooperative adaptive cruise control (cacc)," *IEEE Transactions on Intelligent Transportation Systems*, vol. 17, no. 2, pp. 491–509, 2015.

[3] M. Wang, W. Daamen, S. P. Hoogendoorn, and B. van Arem, "Cooperative car-following control: Distributed algorithm and impact on moving jam features," *IEEE Transactions on Intelligent Transportation Systems*, vol. 17, no. 5, pp. 1459–1471, 2015.

[4] J. K. Hedrick, M. Tomizuka, and P. Varaiya, "Control issues in automated highway systems," *IEEE Control Systems Magazine*, vol. 14, no. 6, pp. 21–32, 1994.

[5] S. E. Shladover, "Longitudinal control of automotive vehicles in close-formation platoons," *Journal of Dynamic Systems, Measurement, and Control*, vol. 113, no. 2, pp. 231–241, 06 1991.

[6] D. Swaroop and J. K. Hedrick, "Constant spacing strategies for platooning in automated highway systems," *Journal of Dynamic Systems, Measurement, and Control*, vol. 121, no. 3, pp. 462–470, 09 1999.

[7] J. A. Fax and R. M. Murray, "Information flow and cooperative control of vehicle formations," *IEEE Transactions on Automatic Control*, vol. 49, no. 9, pp. 1465–1476, 2004.

[8] Y. Zheng, S. E. Li, K. Li, and L.-Y. Wang, "Stability margin improvement of vehicular platoon considering undirected topology and asymmetric control," *IEEE Transactions on Control Systems Technology*, vol. 24, no. 4, pp. 1253–1265, 2015.

[9] E. Shaw and J. K. Hedrick, "String stability analysis for heterogeneous vehicle strings," in *2007 American control conference*. IEEE, Conference Proceedings, pp. 3118–3125.

[10] R. Kianfar, B. Augusto, A. Ebadighajari, U. Hakeem, J. Nilsson, A. Raza, R. S. Tabar, N. V. Irukulapati, C. Englund, and P. Falcone, "Design and experimental validation of a cooperative driving system in the grand cooperative driving challenge," *IEEE Transactions on Intelligent Transportation Systems*, vol. 13, no. 3, pp. 994–1007, 2012.

[11] T. Robinson, E. Chan, and E. Coelingh, "Operating platoons on public motorways: An introduction to the sartre platooning programme," in *17th World Congress on Intelligent Transport Systems*, vol. 1, Conference Proceedings, p. 12.

[12] S. Tsugawa, S. Kato, and K. Aoki, "An automated truck platoon for energy saving," in *2011 IEEE/RSJ International Conference on Intelligent Robots and Systems*. IEEE, Conference Proceedings, pp. 4109–4114.

[13] J. Busch and D. Bestle, "Optimisation of lateral car dynamics taking into account parameter uncertainties," *Vehicle System Dynamics*, vol. 52, no. 2, pp. 166–185, 2014.

[14] P. Vegendla, T. Sofu, R. Saha, M. M. Kumar, and L.-K. Hwang, "Investigation of aerodynamic influence on truck platooning," SAE Technical Paper, Report 0148-7191, 2015.

[15] J. Lan and D. Zhao, "Min-max model predictive vehicle platooning with communication delay," *IEEE Transactions on Vehicular Technology*, vol. 69, no. 11, pp. 12 570–12 584, 2020.

[16] N. Chen, M. Wang, T. Alkim, and B. van Arem, "A robust longitudinal control strategy of platoons under model uncertainties and time delays," *Journal of Advanced Transportation*, vol. 2018, 2018.

[17] E. F. Camacho and C. B. Alba, *Model Predictive Control*. Springer science business media, 2013.

[18] W. B. Dunbar and R. M. Murray, "Distributed receding horizon control for multi-vehicle formation stabilization," *Automatica*, vol. 42, no. 4, pp. 549–558, 2006.

[19] H. Li, Y. Shi, and W. Yan, "Distributed receding horizon control of constrained nonlinear vehicle formations with guaranteed -gain stability," *Automatica*, vol. 68, pp. 148–154, 2016.

[20] P. J. Campo and M. Morari, "Robust model predictive control," in *1987 American Control Conference*. IEEE, Conference Proceedings, pp. 1021–1026.

[21] A. Mesbah, "Stochastic model predictive control: An overview and perspectives for future research," *IEEE Control Systems Magazine*, vol. 36, no. 6, pp. 30–44, 2016.

[22] P. Li, M. Wendt, and G. Wozny, "A probabilistically constrained model predictive controller," *Automatica*, vol. 38, no. 7, pp. 1171–1176, 2002.

[23] Z. Ju, H. Zhang, and Y. Tan, "Distributed stochastic model predictive control for heterogeneous vehicle platoons subject to modeling uncertainties," *IEEE Intelligent Transportation Systems Magazine*, 2021.

[24] V. Turri, B. Besselink, and K. H. Johansson, "Cooperative look-ahead control for fuel-efficient and safe heavy-duty vehicle platooning," *IEEE Transactions on Control Systems Technology*, vol. 25, no. 1, pp. 12–28, 2016.

[25] V. S. Dolk, J. Ploeg, and W. M. H. Heemels, "Event-triggered control for string-stable vehicle platooning," *IEEE Transactions on Intelligent Transportation Systems*, vol. 18, no. 12, pp. 3486–3500, 2017.
[26] A. Alam, J. Mårtensson, and K. H. Johansson, "Look-ahead cruise control for heavy duty vehicle platooning," in *16th International IEEE Conference on Intelligent Transportation Systems (ITSC 2013)*. IEEE, Conference Proceedings, pp. 928–935.
[27] S. Baldi, D. Liu, V. Jain, and W. Yu, "Establishing platoons of bidirectional cooperative vehicles with engine limits and uncertain dynamics," *IEEE Transactions on Intelligent Transportation Systems*, vol. 22, no. 5, pp. 2679–2691, 2020.
[28] G. Wu, G. Chen, H. Zhang, and C. Huang, "Fully distributed event-triggered vehicular platooning with actuator uncertainties," *IEEE Transactions on Vehicular Technology*, 2021.
[29] S. E. Li, F. Gao, K. Li, L.-Y. Wang, K. You, and D. Cao, "Robust longitudinal control of multi-vehicle systems—a distributed h-infinity method," *IEEE Transactions on Intelligent Transportation Systems*, vol. 19, no. 9, pp. 2779–2788, 2017.
[30] G. Taguchi, "Taguchi on Robust Technology Development: Bringing Quality Engineering Upstream," 1993.
[31] X. Du and W. Chen, "Efficient uncertainty analysis methods for multidisciplinary robust design," *AIAA journal*, vol. 40, no. 3, pp. 545–552, 2002.
[32] B. Huang and X. Du, "Analytical robustness assessment for robust design," *Structural and Multidisciplinary Optimization*, vol. 34, no. 2, pp. 123–137, 2007.
[33] G. Taguchi, "Quality engineering (taguchi methods) for the development of electronic circuit technology," *IEEE Transactions on Reliability*, vol. 44, no. 2, pp. 225–229, 1995.
[34] W. Chen, J. K. Allen, K.-L. Tsui, and F. Mistree, "A procedure for robust design: minimizing variations caused by noise factors and control factors," *Journal of Mechanical Design*, vol. 118, no. 4, pp. 478–485, 12 1996.
[35] J. Yin and X. Du, "A safety factor method for reliability-based component design," *Journal of Mechanical Design*, vol. 143, no. 9, p. 091705, 2021.
[36] D. Shen, J. Yin, X. Du, and L. Li, "Distributed nonlinear model predictive control for heterogeneous vehicle platoons under uncertainty," in *2021 IEEE International Intelligent Transportation Systems Conference (ITSC)*, 2021, pp. 3596–3603.
[37] F. S. Wong, "First-order, second-moment methods," *Computers Structures*, vol. 20, no. 4, pp. 779–791, 1985.
[38] J. Yin and X. Du, "High-dimensional reliability method accounting for important and unimportant input variables," *Journal of Mechanical Design*, pp. 1–28, 2021.
[39] S. Darbha and K. Rajagopal, "Information flow and its relation to the stability of the motion of vehicles in a rigid formation," in *Proceedings of the 2005 American Control Conference*. IEEE, Conference Proceedings, pp. 1853–1858.
[40] F. Gustafsson, "Slip-based tire-road friction estimation," *Automatica*, vol. 33, no. 6, pp. 1087–1099, 1997.
[41] S. Song, K. Min, J. Park, H. Kim, and K. Huh, "Estimating the maximum road friction coefficient with uncertainty using deep learning," in *the 21st International Conference on Intelligent Transportation Systems (ITSC 2018)*. IEEE, 2018, pp. 3156–3161.
[42] E. Vanmarcke, *Random Fields: Analysis and Synthesis*. World scientific, 2010.
[43] H. Stark and J. W. Woods, *Probability, Random Processes, and Estimation Theory for Engineers*. Prentice-Hall, Inc., 1986.
[44] K. Worthmann, "Estimates on the prediction horizon length in model predictive control," *IFAC Proceedings Volumes*, vol. 45, no. 17, pp. 232–237, 2012.
[45] S. Vazquez, C. Montero, C. Bordons, and L. G. Franquelo, "Model predictive control of a vsi with long prediction horizon," in *2011 IEEE International Symposium on Industrial Electronics*, Conference Proceedings, pp. 1805–1810.

Jianhua Yin received the B.E. and M.S. degree in Geotechnical Engineering from Chang'an University, Xi'an and Nanjing University, Nanjing, respectively, in China. He is currently pursuing the Ph.D. degree in School of Mechanical engineering, Purdue University, West Lafayette. His current research interests include dimension reduction, machine learning, uncertainty quantification, and design optimization.

Dan Shen (Student Member) received the M.S. degree in Electrical and Computer Engineering from Indiana University-Purdue University Indianapolis (IUPUI), IN, USA, in 2016. He is currently working towards his Ph.D. degree in Electrical and Computer Engineering at Purdue University, West Lafayette, Indiana. His research interests are modeling, state estimation, control, and optimization of complex systems; vehicle active safety systems development and evaluation; combined power energy harvesting systems. He received the 2018 IEEE Intelligent Vehicles Symposium (IV) Best Poster Paper Award (Second Prize).

Xiaoping Du received Ph.D. degree in Mechanical Engineering from the University of Illinois at Chicago in 2002. He joined the Department of Mechanical and Energy Engineering at the Indiana University-Purdue University Indianapolis as a professor in 2019. Prior to that, he was Curator's Distinguished Professor in the Department of Mechanical and Aerospace Engineering at the Missouri University of Science and Technology. His research interests include uncertainty quantification, machine learning, reliability, and design. He has authored/co-authored 120+ research articles in refereed journals. He has served as PI for seven grants from the National Science Foundation and PI/Co-PI for other research projects. He is a fellow of the American Society of Mechanical Engineers. He has received many awards, including Governor's Award for Excellence in Education. He is currently serving as Associate Editor for IISE Transactions and Editor for Structural and Multidisciplinary Optimization.

Lingxi Li (Senior Member) received his Ph.D. degree in Electrical and Computer Engineering from the University of Illinois at Urbana-Champaign in 2008. Since August 2008, he has been with Indiana University-Purdue University Indianapolis (IUPUI) where he is currently professor in electrical and computer engineering. Dr. Li's current research focuses on the modeling, analysis, control, and optimization of complex systems, intelligent transportation systems, connected and automated vehicles, active safety systems, and human factors. He has authored/co-authored over one book and 120+ research articles in refereed journals and conferences, and received two U.S. patents. Dr. Li received a number of awards including four conference best paper awards, outstanding research contributions award, outstanding editorial service award, and university research/teaching awards. He is currently serving as an associate editor for IEEE Transactions on Intelligent Transportation Systems, IEEE Transactions on Intelligent Vehicles, and IEEE Transactions on Computational Social Systems.